

AN UNUSUAL MINI-BAL QUASAR AT $z = 4.59$ ¹

CHRISTOPHER W. CHURCHILL², DONALD P. SCHNEIDER²,
 MAARTEN SCHMIDT³, AND JAMES E. GUNN⁴

² Department of Astronomy and Astrophysics, Pennsylvania State University, University Park, PA 16802

³ California Institute of Technology, Pasadena, CA 91125

⁴ Princeton University Observatory, Princeton, NJ 08544

The Astronomical Journal, in press

ABSTRACT

The $z = 4.591$ quasar PC 1415+3408 exhibits very strong associated metal-line absorption from the NV $\lambda\lambda 1238, 1242$, SiIV $\lambda\lambda 1393, 1402$, and CIV $\lambda\lambda 1548, 1550$ doublets spanning the velocity interval $-1700 \leq v \leq 0 \text{ km s}^{-1}$. Also present, are detached absorption troughs in NV and CIV spanning $-5000 \leq v \leq -3000 \text{ km s}^{-1}$; this is characteristic of broad absorption line (BAL) quasars, but the small overall velocity spread suggests that PC 1415+3408 be classified as a “Mini-BAL” quasar. The NV doublet is consistent with black saturation over the velocity interval -1200 to -500 km s^{-1} ; black NV absorption is extraordinary in all classes of quasars at all redshifts. Over this velocity interval, the CIV doublet is severely blended, but also consistent with black saturation. The material over this range of velocity appears to fully occult the continuum source, the broad emission line region, and any material that could give rise to scattered light. In view of a unified scenario for BAL and Mini-BAL absorption, these facts imply that the quasar is being viewed along a preferred direction. On the other hand, the black Mini-BALs in PC 1415+3408 could be explained if the BAL flow has an unusual geometry compared to the population of BAL quasars, and/or the spatial extent of a scattering region is small at the lower velocities ($-1700 \leq v \leq 0 \text{ km s}^{-1}$).

Subject headings: quasars-BALs; quasars-absorption

1. INTRODUCTION

The absorption lines from metals with $z_{\text{abs}} \simeq z_{\text{em}}$ are useful probes of the kinematics and chemical and ionization conditions of the material surrounding quasars, whether the material gives rise to broad absorption lines (BALs) or narrower absorption lines (e.g. Weymann & Williams 1978; Weymann et al. 1979; Briggs et al. 1984; Turnshek 1984; Morris et al. 1986; Anderson et al. 1987; Turnshek 1988; Weymann et al. 1991; Korista et al. 1993; Turnshek 1995; Arav 1996; Turnshek et al. 1996; Turnshek 1997a, 1997b; Hamann 1997; Hamann et al. 1997a, 1997b, 1997c; Barlow & Sargent 1997; Arav et al. 1998). These absorption lines sample environments in which the chemical and ionization conditions have presumably been influenced by the central engine of the quasar active nucleus (see Arav, Shlosman, & Weymann 1997).

BAL gas is thought to be material within $\sim 1 \text{ kpc}$ of the quasar that is undergoing a high velocity outflow, typically -5000 to $-25,000 \text{ km s}^{-1}$ (Turnshek 1988; Weymann et al. 1991). BAL quasars comprise roughly 10% of all quasars (however, see Goodrich 1997; Krolik & Voit 1998), are radio-quiet (Stocke et al. 1992; however, see Becker et al. 1997), and are quiet, or self-absorbed,

in soft X-rays ($h\nu < 2 \text{ keV}$: Kopko, Turnshek, & Espey 1994; Green & Mathur 1996) and hard X-rays ($2 \leq h\nu \leq 10 \text{ keV}$: Gallagher et al. 1999). Though there are many interpretations of these trends, a unified picture has been proposed in which all quasars have BAL flows and that various viewing angles through the outflowing material result in different observed absorption properties. Most unified pictures, as suggested by polarization studies (e.g. Cohen et al. 1995), have the BAL material *originating* from a disk geometry (e.g. Emmering, Blandford, & Shlosman 1992; de Kool & Begelman 1995; Murray et al. 1995).

An apparently rare class of so-called “Mini-BAL” quasars have been identified (Turnshek 1988; Barlow, Hamann, & Sargent 1997). These quasars often exhibit flat-bottomed (but not necessarily black bottomed) absorption profiles with overall velocity spreads less than 2000 km s^{-1} . The relationship between Mini-BAL and BAL quasars is not yet understood. From the point of view of ultraviolet rest-frame (UV) spectra, Mini-BAL quasars may prove to be the most useful for deducing the chemical and ionization conditions of material involved in BAL flows (Arav 1997), since they do not suffer the extreme blending seen in BAL quasars. Ultimately, how-

¹Based in part on observations obtained at the W. M. Keck Observatory, which is jointly operated by the University of California and the California Institute of Technology.

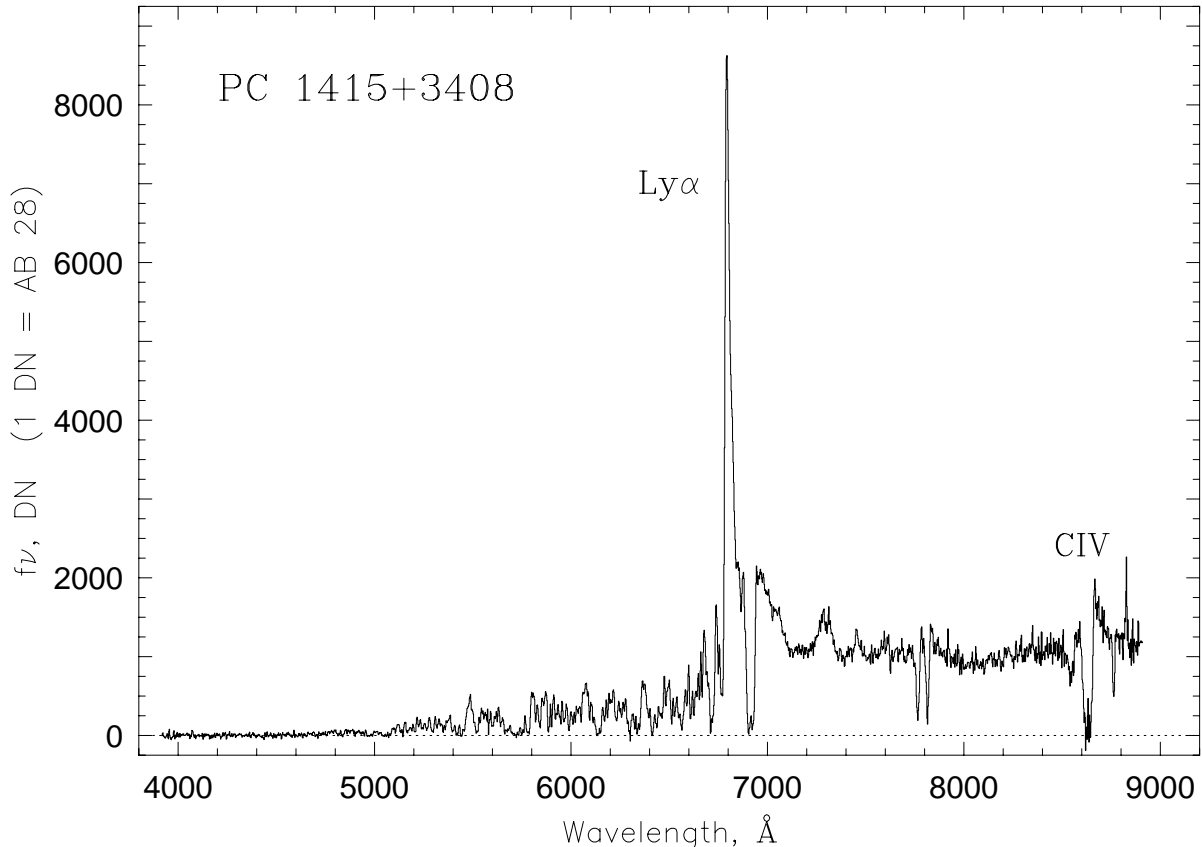


FIG. 1.— LRIS/Keck spectrum of PC 1415+3408 obtained with the 300 lines mm^{-1} grating. The resolution of the data is $R \simeq 900$ (in $0.7''$ seeing using a $1.0''$ slit) with 2.6 \AA pix^{-1} . The unit of flux along the vertical axis is $2.3 \times 10^{-31} \text{ ergs cm}^{-2} \text{ s}^{-1} \text{ Hz}^{-1}$ (= AB magnitude 28).

ever, any working model of BAL flows will need to survive observational probings not only with UV rest-frame data, but with radio and both soft and hard X-ray data as well.

In addition to multi-band observations, studies are needed that extend the sample of BAL and Mini-BAL quasars to the highest redshifts. Nearly 100 quasars at $z \geq 4.0$ have now been discovered and the fraction with BAL features appears to be the same as at lower redshifts (e.g. Storrie-Lombardi et al. 1996). Extending BAL quasar studies to $z > 4$ would yield a chronological baseline on par with studies of the $\text{Ly}\alpha$ absorbers for firmly establishing cosmic evolution (or lack of) in a class of astronomical object. Unlike (but complementary to) studies of $\text{Ly}\alpha$ absorption, investigations of BAL quasars probe the most energetic and active sites in the Universe.

In this paper, we present high-quality spectra of one of the few known $z \geq 4.5$ quasars, PC 1415+3408, which possesses very unusual mini-BAL spectral characteristics. PC 1415+3408 was first reported by Schneider, Schmidt, & Gunn (1997, hereafter SSG97) and was observed to have peculiar emission and/or absorption features as seen in a low-resolution ($\sim 25 \text{ \AA}$) and low signal-to-noise spectrum. Furthermore, an accurate emission redshift measurement was difficult; they tentatively as-

signed $z_{\text{em}} = 4.6$, but noted that the complex CIV emission profile could be placed at $z_{\text{em}} = 4.76$. We present a robust emission redshift and investigate the emission and absorption line properties of PC 1415+3408. Throughout this work we assume $H_0 = 50 \text{ km s}^{-1} \text{ Mpc}^{-1}$, $q_0 = 0.5$. We do not make a distinction between the categorical terms “associated” and “intrinsic” absorption for describing material with $z_{\text{abs}} \simeq z_{\text{em}}$ (for a clear exposition see Barlow, Hamann, & Sargent 1997).

2. SPECTROSCOPIC OBSERVATIONS

Spectra of PC 1415+3408 were acquired with the Low Resolution Imaging Spectrograph (LRIS) on the Keck I Telescope (Oke et al. 1995). An 1800 second exposure was obtained on 1996 April 14, using the 1200 line mm^{-1} grating and a $0.7''$ slit under $\sim 1''$ seeing conditions. The resolution of the spectrum is $R \sim 4000$ with $\sim 0.64 \text{ \AA pix}^{-1}$, and the wavelength coverage is $5797.6\text{--}7108.8 \text{ \AA}$. An additional 1800 second exposure using the 300 line mm^{-1} grating with a $1.0''$ slit was obtained on 1997 April 3. The seeing was $\sim 0.7''$, resulting in a resolution of $R \sim 900$ with $\sim 2.4 \text{ \AA pix}^{-1}$. The wavelength coverage is $3917.8\text{--}8908.9 \text{ \AA}$. For all observations, the spectrograph slit was set at the parallactic angle to minimize differential refraction. The spatial scale on the CCD is $0.213'' \text{ pix}^{-1}$.

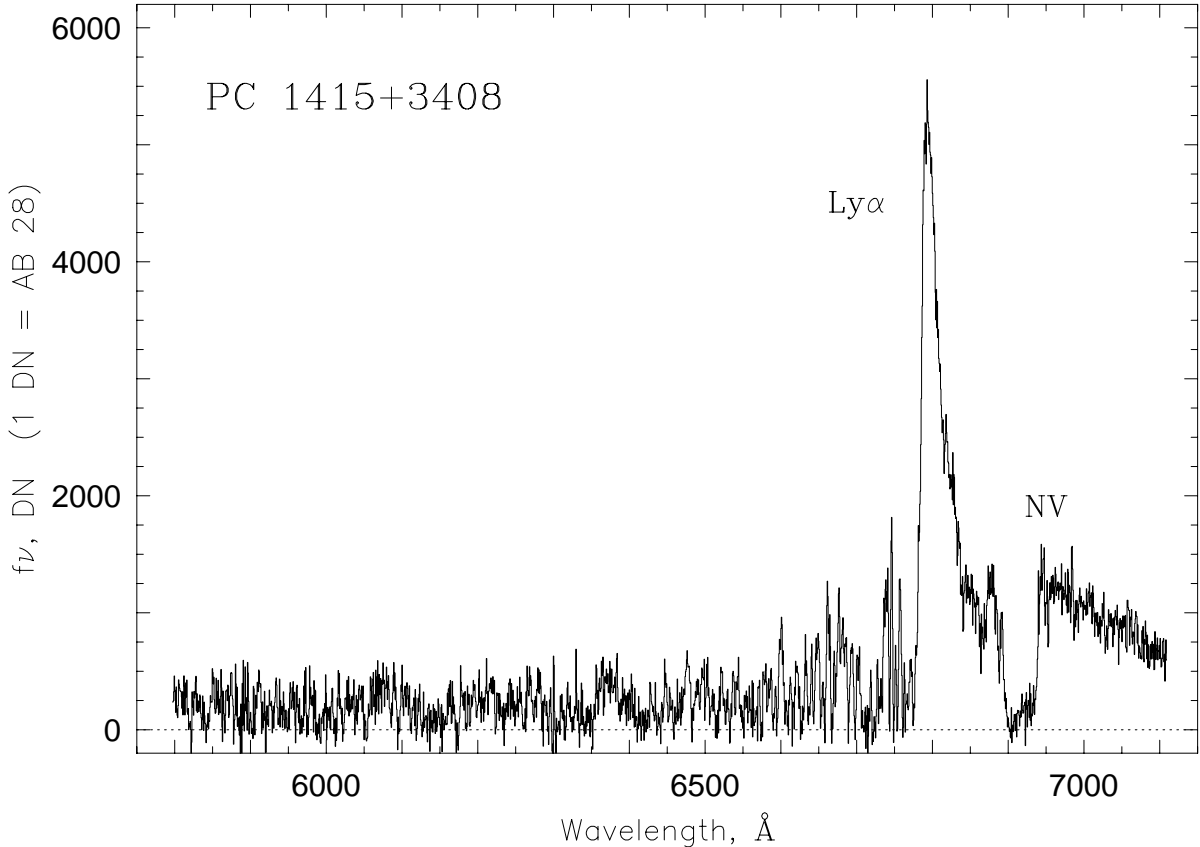


FIG. 2.— LRIS/Keck spectrum of PC 1415+3408 obtained with the 1200 lines mm^{-1} grating. The resolution of the data is $R \simeq 4000$ with $0.65 \text{ \AA pix}^{-1}$.

The raw data frames were processed in the standard fashion, including bias subtraction and flat fielding. The spectra were extracted using the optimal algorithm of Horne (1986). The wavelength scale was set (for both gratings) with cubic fits to lines from Hg, Kr, and Ar discharge lamps. The resulting RMS errors are 0.09 \AA for the 1200 lines mm^{-1} grating and 0.23 \AA for the 300 lines mm^{-1} grating. For the latter observations, the seeing was less than the slit width, resulting in a ~ 1 pixel uncertainty in the wavelength scale zero point. The flux calibration and the removal of atmospheric absorption bands were performed using the flux standards of Oke & Gunn (1983). The fully reduced and calibrated spectra are shown in Figure 1 (300 lines mm^{-1}) and Figure 2 (1200 lines mm^{-1}).

3. PC 1415+3408

3.1. UV Rest-Frame Properties

In Figure 3 we show the 300 lines mm^{-1} spectrum redward of the $\text{Ly}\alpha$ emission line with the vertical scale set to emphasize the continuum features. PC 1415+3408 has strong, broad high-ionization emission lines from $\text{NV } \lambda 1240.1$, $\text{SiIV+OIV } \lambda 1400.0$, and $\text{CIV } \lambda 1549.1$. The cores and blue wings of these emission lines are strongly absorbed. In absorption,

the $\text{NV } \lambda\lambda 1238, 1242$ doublet members are partially resolved, the $\text{SiIV } \lambda\lambda 1393, 1402$ doublet members are well resolved, and the $\text{CIV } \lambda\lambda 1548, 1550$ doublet members are fully blended. There are also weaker, low-ionization emission lines from $\text{SiII } \lambda 1263.0$, $\text{OI+SiII } \lambda 1304.5$, and $\text{CII } \lambda 1334.5$. The SiII emission is on the red wing of the broad NV emission line, making it difficult to accurately determine the SiII strength. The OI+SiII feature appears to be among the strongest seen in quasars (of all redshifts) reported in the literature and has a weak absorption feature that is slightly redshifted. As seen in Figure 1, there is a clear Lyman limit break at 5080 \AA , which corresponds to $z = 4.575$. The lack of a recovery by 704 \AA in the rest-frame implies $N(\text{HI}) > 10^{18.2} \text{ cm}^{-2}$. There is strong $\text{Ly}\alpha$ absorption at 6777 \AA that corresponds to the break (see Figures 1 and 2). In Table 1, we list the overall properties of PC 1415+3408. The g_4 and r_4 filters each have widths of approximately 450 \AA and are centered at 4930 and 6550 \AA , respectively. The quantity AB_{1450} is the observed AB magnitude, corrected for Galactic reddening, at $\lambda = 1450(1+z)$, where $AB = -2.5 \log f_\nu - 48.60$ (see Schneider, Schmidt, & Gunn 1989).

The spectral energy index, α , was determined by fitting the function $f_\nu \propto \nu^\alpha$ to interactively selected continuum points redward of $\sim 6780 \text{ \AA}$ using the 300 lines mm^{-1}

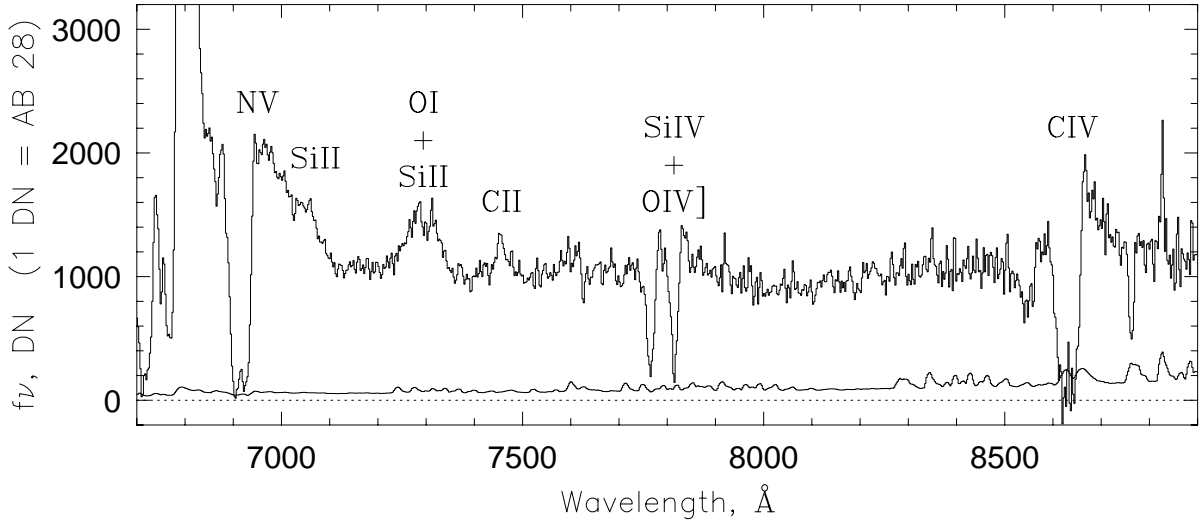


FIG. 3.— The 300 lines mm^{-1} spectrum of PC 1415+3408 redward of $\text{Ly}\alpha$ emission. The broad emission lines are labeled. The narrow “absorption” line at 8762 Å and the narrow “emission” lines at 8827 Å and on the CIV broad emission line at 8670 Å are artifacts of the sky subtraction. The 1σ error array is given by the spectrum just above the zero point.

spectrum. A possible observational systematic error in the slope could be differential refraction, though we note that the seeing was better than the projected width of the slit and we aligned the slit with the parallactic angle. To estimate possible systematics in the fitting procedure itself, we performed multiple interactive fits. Just over 65% of the total available wavelength coverage redward of the blended $\text{Ly}\alpha+\text{NV}$ emission line was employed. This exercise yielded $\alpha = -0.45 \pm 0.05$. Our α value is significantly different than that measured by SSG97 ($\alpha = -1.2$) using lower quality data. Normalization of the power law gives $AB_{1450} = 20.6$, from which an absolute blue-band magnitude of $M_B = -25.9$ was calculated following Schneider et al. (1989)². These values are in good agreement with those calculated by SSG97.

Measurements of the emission line properties were obtained by interactively fitting a smooth third-order Legendre polynomial to the “source” continuum redward of 6770 Å, excluding emission and absorption lines. The emission lines were modeled with single component Gaussian fits using a Levenberg–Marquardt least square minimizer (More 1978). However, the $\text{Ly}\alpha+\text{NV}$ blend required three Gaussian components. Each component fit yielded a central wavelength, width, equivalent width, and 1σ uncertainties in these quantities. The resulting emission line profiles are shown in Figure 4, and their measured properties are listed in Table 2. A redshift of $z_{\text{em}} = 4.591 \pm 0.001$ was determined from the weighted mean of the emission line central wavelengths (corrected to vacuum). The weight for each line was taken to be σ_λ^{-2} , where σ_λ is the 1σ uncertainty in the central wavelength. The blended $\text{Ly}\alpha+\text{NV}$ emission line was excluded.

The quantity $\Delta\text{Ly}\alpha$, given by $[\lambda_{\text{Ly}\alpha}/(1 + z_{\text{em}}) - 1215.67]$, where $\lambda_{\text{Ly}\alpha}$ is the vacuum corrected wavelength of the $\text{Ly}\alpha$ emission peak, quantifies the degree of blueward absorption in the rest-frame of the $\text{Ly}\alpha$ emission line. The offset measured for PC 1415+3408, $\Delta\text{Ly}\alpha = 0.8$ Å, is the smallest measured at $z \geq 4$ as compared to the sample of 33 quasars (of which 13 were $z \geq 4$) studied by Schneider, Schmidt, & Gunn (1991) [also see Sargent, Boksenberg, & Steidel 1988]. This small $\Delta\text{Ly}\alpha$ implies either that the $\text{Ly}\alpha$ emission line is intrinsically very narrow or suffers absorption along both wings ($\text{Ly}\alpha$ to the blue and high velocity, asymmetric, NV to the red) that conspire to leave its peak relatively unshifted.

For the highest redshift quasars, absorption blueward of $\text{Ly}\alpha$ emission is very strong. The “flux deficit” (Oke & Korytcanski 1982), given by

$$D = \left\langle 1 - \frac{f_\nu(\text{observed})}{f_\nu(\text{continuum})} \right\rangle, \quad (1)$$

provides a quantitative measure of this absorption, where $f_\nu(\text{observed})$ is the observed flux and $f_\nu(\text{continuum})$ is the predicted unattenuated flux based upon extrapolation of the spectral energy index. This deficit is measure over two regimes. The first, D_A , is measured from 1050 to 1170 Å in the rest-frame of the quasar and gives the mean absorption blueward of the $\text{Ly}\alpha$ emission line and redward of the $\text{Ly}\beta+\text{OVI}$ emission line; it is designed to measure $\text{Ly}\alpha$ -only absorption. The second, D_B , is measured from 920 to 1015 Å in the rest-frame of the quasar and gives the mean absorption blueward of the $\text{Ly}\beta+\text{OVI}$ emission line and redward of the Lyman limit

²The zero-point offset applied here is corrected to be half that applied in their work (see Schmidt, Schneider, & Gunn 1995).

of the quasar.

The dominant source of error in the measurement of the flux decrement is the uncertainty in the power-law continuum fit. To estimate the uncertainty in our measurement, we used the 1σ spread in α and in AB_{1450} that conspire to give the extreme upper and lower values of D . For PC 1415+3408, we measured $D_A \simeq 0.7$, with an uncertainty of 0.06. This value is typical of $z \simeq 4.5$ quasars; D_A is seen to rise from $\sim 50\%$ at $z = 4$ to $\sim 80\%$ at $z \sim 5$ (Schneider, Schmidt, & Gunn 1991). This has been shown to be consistent with an increase in the numbers of Ly α clouds at higher redshifts (Giallongo & Cristiani 1990; Jenkins & Ostriker 1991; Schneider, Schmidt, & Gunn 1991). We find $D_B \simeq 0.8$, with uncertainty 0.1. This value is slightly high compared to the mean value 0.65 measured for 13 $z > 4$ non-BAL quasars (Schneider, Schmidt, & Gunn 1991), possibly due to strong associated metal lines (esp. O VI, C III, N III).

In the 300 lines mm^{-1} spectrum (see Figure 1), there is strong, broad absorption at 6143 \AA , which has the appearance of a damped Ly α absorber (DLA) at $z = 4.054$. If this is a DLA, the rest-frame equivalent width for Ly α is $14.5 \pm 0.6 \text{ \AA}$, which corresponds to $\log N(\text{H I}) \sim 21.0 \text{ cm}^{-2}$. However, in the 1200 lines mm^{-1} spectrum, the absorption appears to break into a series of smaller, blended Ly α clouds, as seen in Figure 2. This serves as a warning that DLA candidates at $z \sim 4$ in spectra with 5–6 \AA resolution require follow-up verification at higher resolutions.

3.2. Radio and X-ray Properties

PC 1415+3408 is not detected in the FIRST survey to a flux limit $f_\nu(1.4 \text{ GHz}) \leq 1.0 \text{ mJy}$. Assuming a spectral power index of $\alpha = -0.5$ for both the radio and optical bands, we obtained $L_\nu(6\text{cm}) \leq 10^{25.2} \text{ W Hz}^{-1}$ and $L_\nu(4400 \text{ \AA}) = 10^{24.0} \text{ W Hz}^{-1}$ for an isotropically radiating point source. Using $L_\nu(6\text{cm}) \simeq 10^{25} \text{ W Hz}^{-1}$ as the dividing line between radio-loud and radio-quiet quasars (Kellerman et al. 1989), PC 1415+3408 is at most a radio-moderate quasar. Another indicator for radio-loudness, $R = L_\nu(6\text{cm})/L_\nu(4400 \text{ \AA})$, is less than $\simeq 15$, which also suggests a radio-moderate quasar at most (Kellerman et al. 1994). If the radio spectrum is flat ($\alpha = 0$), the upper limit on the radio luminosity decreases by 30%. PC 1415+3408 is clearly not a radio-loud quasar. Even if no BAL absorption was seen in PC 1415+3408, it is statistically likely to be radio quiet, given that only 5–10% of optically selected quasars are radio loud at high redshifts (e.g. Schmidt et al. 1995, and references therein).

In the X-ray band, there are no serendipitous or pointed observations of PC 1415+3408 by either *ROSAT* or *ASCA*, though an upper limit of $0.05 \text{ counts s}^{-1}$ was obtained

from the *ROSAT Bright Source Catalog*. Radio-quiet quasars have $\alpha_{\text{ox}} = -1.57 \pm 0.15$ (Green et al. 1995), where $\alpha_{\text{ox}} = 0.348 \log[L_\nu(2500 \text{ \AA})/L_\nu(2 \text{ keV})]$. Assuming this value of α_{ox} , an isotropically radiating point source, an X-ray energy index of $\alpha_E = -1$, and a Galactic hydrogen column density of $N(\text{H I}) = 1.3 \times 10^{20} \text{ cm}^{-2}$ toward PC 1415+3408 (Stark et al. 1992), we calculated

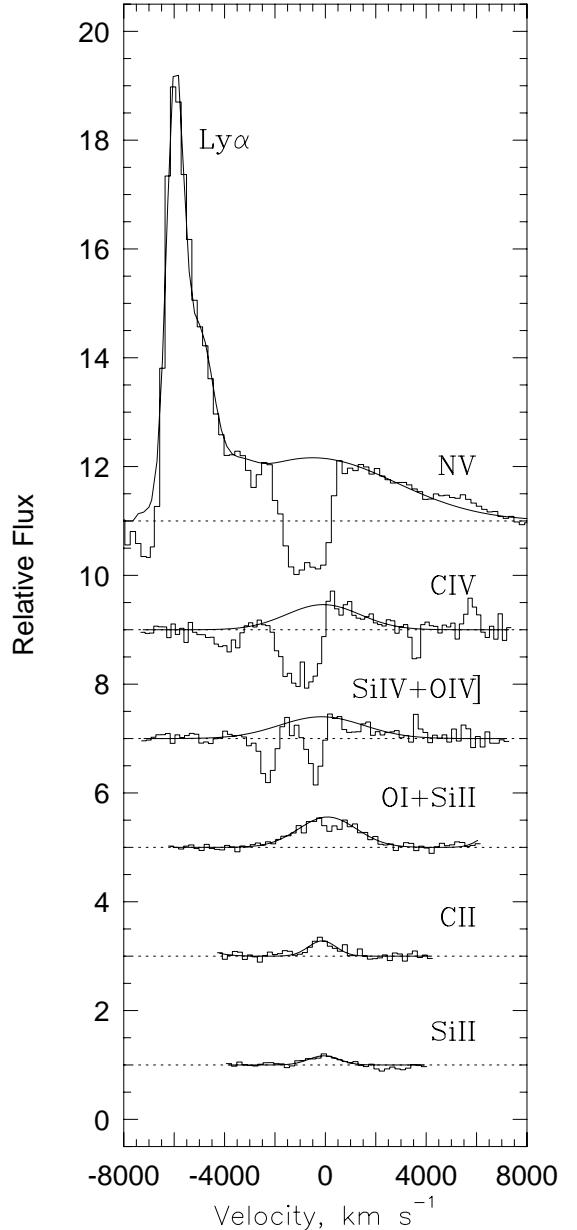


FIG. 4— The emission lines and the NV, CIV, and SiIV absorption lines of PC 1415+3408 as measured in the 300 lines mm^{-1} grating spectrum. For presentation, the spectra have been normalized by the “source” continuum, are offset vertically by a factor of two (the respective zero points are 0, 2, 4, 6, 8, and 10), and are aligned in velocity referenced to the quasar emission redshift.

TABLE 1
PROPERTIES OF PC 1415 + 3408

Parameter	Value
Right ascension (1950.0)	14 ^h 15 ^m 46.6 ^s
Declination (1950.0) ...	+34° 08' 30"
z_{em}	4.591 ± 0.001
g_4	23.76 ± 0.17
r_4	21.37 ± 0.08
α	-0.45 ± 0.05
AB_{1450}	20.57 ± 0.09
M_{1450}	-26.3
M_B	-25.9
D_A	0.70 ± 0.06
D_B	0.8 ± 0.1
$\Delta\text{Ly}\alpha$	$0.81 \pm 0.02 \text{ \AA}$

an expected X-ray luminosity of $L_\nu(2 \text{ keV}) = 8.5 \times 10^{22} \text{ W Hz}^{-1}$ using PIMMS (Mukai 1997). This is an order of magnitude below the upper limit on $L_\nu(2 \text{ keV})$ from the *ROSAT Bright Source Catalog*.

4. THE ASSOCIATED BROAD ABSORPTION LINES

As seen in Figures 1–3, strong, broad absorption is present in the cores of the three high ionization emission lines. The velocity alignment of these absorption features is shown in Figure 4. Over the the velocity interval -1700 to $\sim 0 \text{ km s}^{-1}$, the NV and CIV doublets are blended, but the two members of the SiIV doublet are resolved. Both NV and CIV are consistent with “black” saturation (\sim zero flux) over the velocity range -1200 to -500 km s^{-1} . An additional component, or “secondary detached trough”, is evident at velocities from -2200 to -3500 km s^{-1} for NV and from -3000 to -5000 km s^{-1} for CIV. In broad absorption line (BAL) quasars, “double-trough” broad absorption is not uncommon, appearing $\sim 20\%$ of the time (Weymann et al. 1991; Korista et al. 1993).

That the broad absorption lines in PC 1415+3408 have $z_{\text{abs}} \simeq z_{\text{em}}$ is highly suggestive that they are physically associated with the quasar, that they do not arise in intervening objects. Furthermore, there are other features that suggest the lines are associated with the quasar. The lines are characteristic of BAL flow in that they (1) are smoothed bottomed and do not exhibit the complex kinematic structure observed in galaxy halos, (2) are comprised of a primary and a detached trough, a common feature of BALs, and (3) are significantly broader than the $\leq 600 \text{ km s}^{-1}$ velocity spreads of galactic halos. Since the CIV absorption extends to less than 5000 km s^{-1} from the

emission redshift (Weymann et al. 1991), PC 1415+3408 should be classified as a so-called “Mini-BAL” quasar (e.g. Turnshek 1988; Barlow, Hamann, & Sargent 1997). Examples of Mini-BAL quasars are Q 0449–13 at $z_{\text{em}} = 3.09$ (Barlow, Hamann, & Sargent 1997) and the $z_{\text{em}} = 1.98$ radio-loud quasar PHL 1157+0128 (Aldcroft, Bechtold, & Foltz 1997). The CIV profile of the latter is virtually identical to that of PC 1415+3408, except that the secondary trough is centered at -5100 km s^{-1} and has a spread of $\simeq 1900 \text{ km s}^{-1}$.

In Figure 5, we show the $4900\text{--}6100 \text{ \AA}$ region of the $300 \text{ lines mm}^{-1}$ spectrum. Bar ticks mark the expected wavelength regions of Ly γ , CIII $\lambda 977$, NIII $\lambda 989$, Ly β , and OVI $\lambda\lambda 1031, 1037$, based upon the $-5000 \leq v \leq -3000$ and the $-1700 \leq v \leq 0 \text{ km s}^{-1}$ absorption troughs of CIV. Higher velocity absorption is evident in the Ly β and OVI blend spanning 5700 to 5800 \AA ; the blue wing is consistent with the detached trough of the CIV. The SVI $\lambda\lambda 933, 944$ doublet may be present, but heavily blended by the Lyman series. The presence of PV $\lambda\lambda 1117, 1128$, sometimes seen in BAL quasars, is ambiguous.

4.1. Exploring the Kinematics

For the remainder of this section, we focus on the primary absorption, that in the velocity range $-1700 \leq v \leq 0 \text{ km s}^{-1}$. In Figure 6, we show the absorption blueward of the Ly α emission line (upper panel) and of the blended NV doublet (lower panel), as measured in the $1200 \text{ line mm}^{-1}$ spectrum. The data are aligned in the rest-frame velocity of the quasar. The quasar continuum blueward of Ly α emission was estimated by extrapolating a two-component Gaussian fit to the Ly α +NV blend

TABLE 2
EMISSION LINE PROPERTIES OF PC 1415 + 3408

Tran	λ_r , Å	λ_o , Å	z_{em}	W_o , Å	W_r , Å	σ_r , Å
Ly α + Nv ^a .	1215.7 + 1240.1	6792.4 \pm 0.1	4.589	448 \pm 45	80.1 \pm 8.0	1.23 \pm 0.02
SiII	1263.0	7060.5 \pm 0.7	4.592 \pm 0.001	8.1 \pm 0.4	1.45 \pm 0.07	2.83 \pm 0.09
OI + SiII ..	1304.5	7294.3 \pm 1.4	4.593 \pm 0.001	39.3 \pm 3.4	7.03 \pm 0.60	5.00 \pm 0.27
CII	1334.5	7456.3 \pm 1.7	4.589 \pm 0.001	9.8 \pm 1.5	1.76 \pm 0.27	2.48 \pm 0.30
SiIV + OIV]	1400.0	7814.4 \pm 4.3	4.583 \pm 0.003	41.1 \pm 5.8	7.35 \pm 1.04	7.67 \pm 0.73
CIV	1549.1	8657.5 \pm 6.9	4.590 \pm 0.004	45.6 \pm 11.9	8.15 \pm 2.12	7.95 \pm 1.06

^aThe central wavelength quoted is that of the narrow peak of the Ly α line.

with an underlying power law using the fiducial spectral energy index, $\alpha = -0.5$ (since our value of -0.45 is consistent with this fiducial value). The resulting continuum is shown as a dot-dot curve in Figure 6.

A series of Gaussians was fit to the flux values in the Ly α absorption just blueward Ly α emission. The free parameters for each Gaussian are the central wavelength, amplitude, and width (unless the width of the component, σ_c , is less than the instrumental resolution; in this case σ_c is set to $\lambda_c/(2.35R)$, where λ_c is the component centroid and $R = 4000$ is the spectrum resolution). We started with a two-component fit and increased the number of components until a standard F-test yielded no further significant gain (98% confidence level) in the “goodness” of the fit, as measured by the reduced χ^2 . Our adopted fit has five Gaussian components. Although these five Ly α com-

ponents are not to be taken literally as distinct absorbers, we emphasize the excellent alignment in velocity with the blended Nv doublet. In the bottom panel of Figure 6, we transpose the ticks from the Ly α decomposition to the Nv doublet (upper ticks denote the $\lambda 1238$ transition and lower ticks denote the $\lambda 1242$ transition); this alignment is strongly suggestive that the Ly α absorption is metal-rich and gives rise to the Nv.

In Figure 7, we present the Ly α and Nv absorption (both the 1200 and 300 lines mm^{-1} spectra are shown), and the SiIV and CIV absorption in the 300 lines mm^{-1} spectrum. Both resolutions of the Ly α and Nv are displayed so that the relative quality of the SiIV and CIV data can be judged. The profiles are aligned in velocity with the zero point set by the stronger member of each doublet with respect to the quasar emission redshift. The

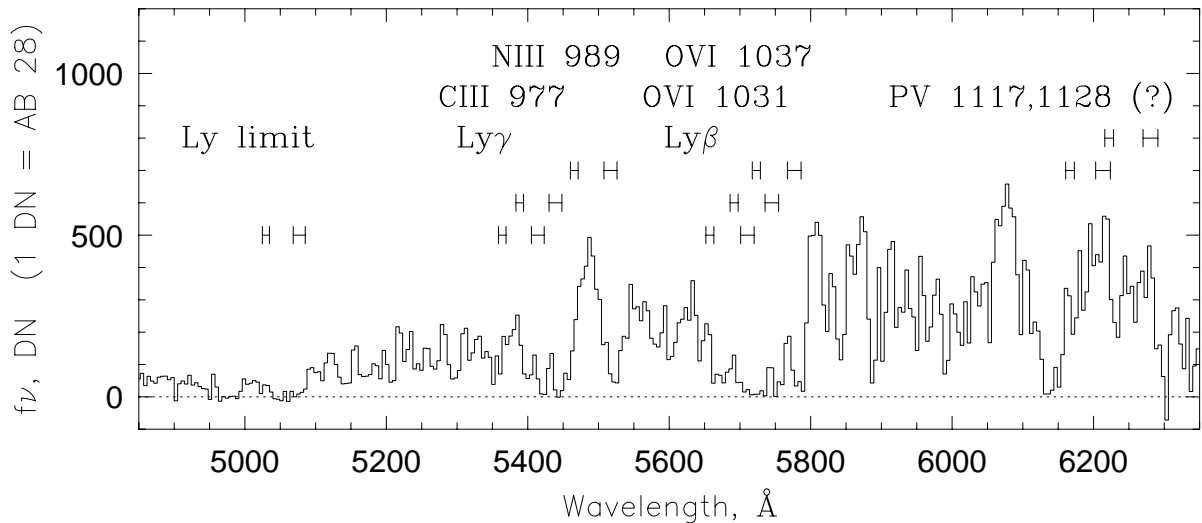


FIG. 5.— The 300 lines mm^{-1} spectrum of PC 1415+3408 blueward of Ly α emission. A significant portion of the absorption amongst the Ly α forest is due to associated absorption from Ly γ +CIII, NIII, and Ly β +OVI. The labeled bar ticks give the expected wavelength regions of these species based upon the velocity spreads of Ly α and Nv.

data are continuum normalized for presentation.

4.2. Covering Fraction of the Absorbing Material

The observations suggest that the absorbing gas highlighted in Figure 7 is outflowing material originating in the immediate environment of the quasar. There are several examples where such material does not fully occult the broad emission line region and/or of the quasar continuum source (e.g. Barlow & Sargent 1997). Here, we investigate the possibility that the BAL flow material associated with PC 1415+3408 partially covers the emission source(s).

If τ is the effective optical depth of an absorbing cloud that occults a fraction, C_f , of the source, the residual intensity, R , in normalized units is,

$$R(\lambda) = \{1 - C_f(\lambda)\} + C_f(\lambda)e^{-\tau(\lambda)}, \quad (2)$$

where the first term on the right-hand side represents unocculted photons and the second term represents unabsorbed photons. For a doublet, the covering factor can be obtained as the solution to

$$\left\{ \frac{R_r - 1 + C_f}{C_f} \right\}^{\tau_b/\tau_r} = \left\{ \frac{R_b - 1 + C_f}{C_f} \right\}, \quad (3)$$

where $\tau_b/\tau_r = (g_L f_{LU} \lambda)_b / (g_L f_{LU} \lambda)_r$, where g_L is the degeneracy of the lower level, f_{LU} is the oscillator strength of the transition (where L and U denote the lower and upper levels, respectively), and the subscripts b and r denote the blue and red transitions, respectively.

To apply this technique, however, the absorption profiles need to be resolved, for if they are not resolved then smearing from the instrumental spread function destroys the optical depth ratios at each velocity point (see Ganguly et al. 1999). The NV doublet is resolved, though its members are partially blended. Using software kindly provided by R. Ganguly, we computed a covering factor, C_f , of $0.97^{+0.03}_{-0.12}$, over the limited velocity region -1100 to -600 km s $^{-1}$ in the 1200 line mm $^{-1}$ spectrum. The NV absorption is consistent with a unity covering factor. The CIV doublet (300 line mm $^{-1}$ spectrum) is fully blended, and is not viable for the partial covering test.

For the unresolved SiIV profiles, the covering factor can be investigated using Voigt profile (VP) decomposition, which effectively deconvolves the instrumental profile from the optical depth model. In the case of partial covering, VP components cannot be made consistent with both members of the doublet. Since a VP decomposition is a non-unique model, however, any evidence for partial covering using this technique is less conclusive. If a *reasonable* (i.e. physically motivated) VP decomposition can

be made consistent with full coverage, it can tentatively be interpreted that the data are consistent with a unity covering factor.

Using MINFIT (Churchill 1997), which uses Levenberg-Marquardt least square minimization (More 1978) while enforcing a minimum number of components, a VP decomposition of the SiIV doublet yields three components consistent with a unity covering factor. The reduced χ^2 was 1.2. These three components effectively correspond to the five components found in the higher resolution spectrum (see Figure 6), with the central, narrow SiIV VP component corresponding to the

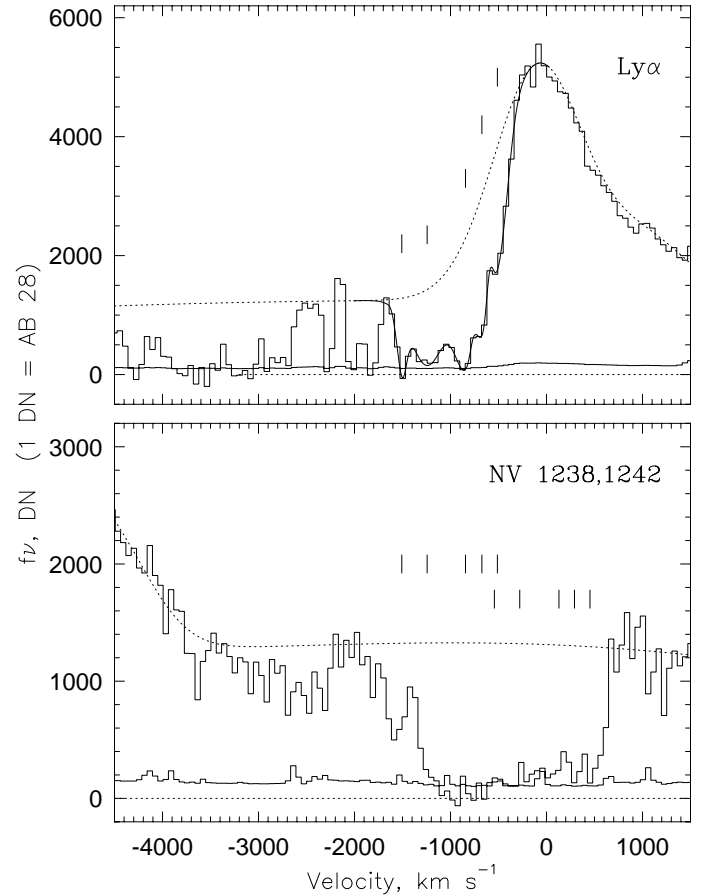


FIG. 6— The associated Ly α (upper panel) and NV $\lambda\lambda 1238, 1242$ (lower panel) absorption of PC 1415+3408 as measured in the 1200 lines mm $^{-1}$ grating spectrum. The velocity zero-point is the quasar redshift, $z_{\text{em}} = 4.591$. The histogram data are the observed flux values and their uncertainties. Five “components” are shown based upon blended Gaussian fitting. Ticks above the continuum give the Gaussian centroids. In order of increasing outflow velocity, the absorption redshifts are $z = 4.5815, 4.5785, 4.5753, 4.5678$, and 4.5629 . The dot-dot lines are rough estimates of the continua and the solid line shows the five-component model.

central $\text{Ly}\alpha$ Gaussian component, and the VP components in the wings of the SiIV each corresponding to two Gaussian components in the wings of the $\text{Ly}\alpha$.

4.3. Lower Limits on Column Densities

Though BAL absorption lines sample dynamically active gas over a wide range of ionization conditions and kinematics, the lines are often heavily blended so that deducing the physical conditions of the gas can be intractable (Arav et al. 1998; however, see Turnšek et al. 1996). In Table 3, we show the lower limits on the column densities using the apparent optical depth (AOD) method (Savage & Sembach 1991). The NV and CIV doublets are both blended and saturated. For the SiIV , the profiles do not drop to zero flux in their cores, but they do exhibit unresolved saturation, as deduced by the factor of two difference in their apparent column densities; as such, the measured SiIV column densities are likely to be significantly underestimated. The data do not allow definitive statements about the metallicities and ionization conditions of the absorbing gas.

5. DISCUSSION

The UV rest-frame absorption associated with PC 1415+3408 exhibits four remarkable properties.

(1) The NV doublet is consistent with black saturation over six resolution elements in a 1.7 \AA resolution spectrum. The doublet is partially blended.

(2) The CIV is consistent with black saturation in a $\sim 8 \text{ \AA}$, lower resolution spectrum.

(3) The $\text{Ly}\alpha$ absorption along the blue wing of the $\text{Ly}\alpha$ emission line is clearly associated with the primary NV and CIV troughs (velocity range $-1700 \leq v \leq 0 \text{ km s}^{-1}$). This $\text{Ly}\alpha$ absorption is neither smooth nor flat bottomed, but exhibits clear structure.

(4) Both CIV and NV have secondary “detached” troughs, and these troughs are not aligned in velocity space; NV is at lower velocities than CIV. The detached troughs have velocity spreads less than 2000 km s^{-1} and smooth, non-zero, flat bottoms.

What makes the absorption in PC 1415+3408 exceptional is that *both* the NV and CIV absorption profiles are consistent with black saturation, even at a spectral resolution of $\sim 8 \text{ \AA}$ ($300 \text{ lines mm}^{-1}$ spectrum). In the $1200 \text{ lines mm}^{-1}$ spectrum (resolution 1.7 \AA), the unblended portion of the NV $\lambda 1238$ transition is consistent with zero flux across six resolution elements. It is unusual for this to occur with CIV [especially in comparable $5\text{--}7 \text{ \AA}$ resolution spectra (e.g. Storrie-Lombardi et al. 1996)] and it is exceedingly rare with NV at all observed resolutions. Interestingly, the Mini-BALs 0835+5804 and PHL 1157+0128 have absorption nearly consistent with

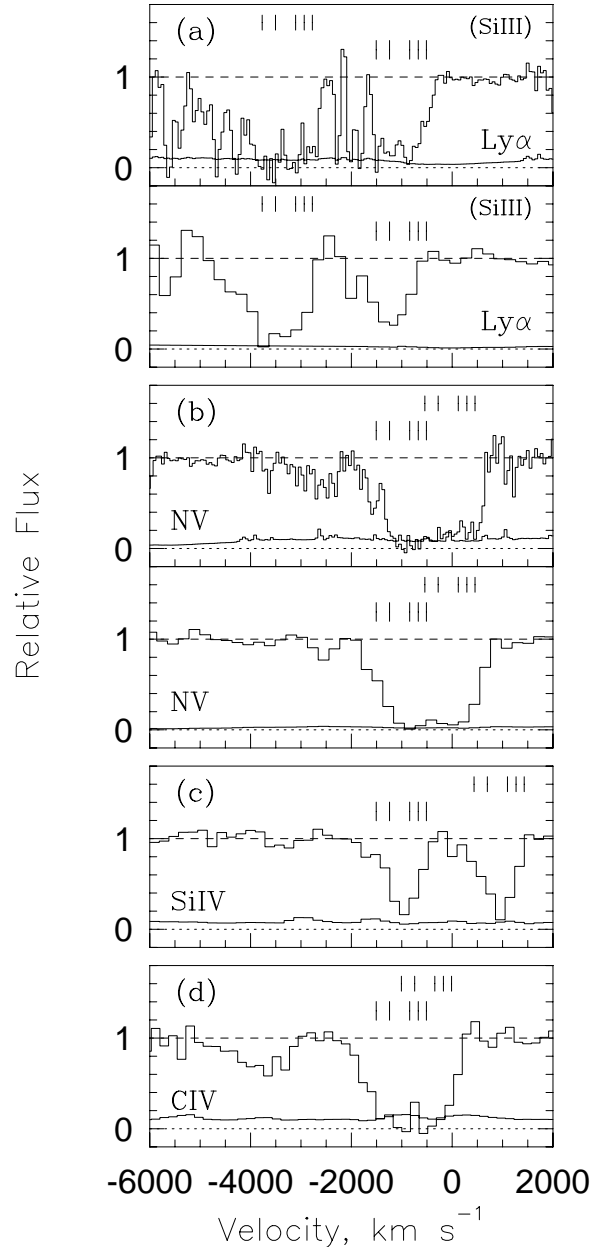


FIG. 7— The $\text{Ly}\alpha$ NV, CIV, and SiIV absorption lines of PC 1415+3408. For $\text{Ly}\alpha$ and NV, both the 1200 and $300 \text{ lines mm}^{-1}$ spectra are presented so that the greater detail at higher resolution can be compared to that at lower resolution. For presentation, the spectra have been normalized by the both the “source” and broad emission line continua and are aligned in velocity space referenced to the quasar emission redshift. Long ticks above the continuum give the velocities of the tentatively suggested components. The red members of the doublets are shown with shorter ticks. In the case of $\text{Ly}\alpha$, the additional ticks show the expected location of $\text{SiIII } \lambda 1206$.

TABLE 3
ABSORPTION LINE PROPERTIES OF PC 1415 + 3408

Ion	$W_r, \text{\AA}$	$\log N_{aod}, \text{cm}^{-2}$	$(v^-, v^+), \text{km s}^{-1}$
H I ^a	3.7 ± 0.3	> 18.2	$(-2700, -200)$
N V 1239 ^b	5.3 ± 0.2	$> 15.7^c$	$(-2200, -400)$
C IV 1548	5.5 ± 0.9	$> 15.4^c$	$(-2300, +100)$
Si IV 1394	2.7 ± 0.3	14.7^d	$(-1900, -600)$
Si IV 1402	2.9 ± 0.3	15.0^d	$(-1900, -600)$

^aThe tabulated column density is based upon Lyman limit break in 300 line mm^{-1} spectrum (see text). The apparent optical depth method yielded $\log N_{aod}(\text{H I}) > 15.3 \text{ cm}^{-2}$.

^bMeasured from the 1200 line mm^{-1} spectrum.

^cAmbiguity due to doublet blending. A unity doublet ratio has been assumed.

^dThese column densities should be considered lower limits due to unresolved saturation.

being black (Aldcroft, Bechtold, & Foltz 1997). Though the velocity spreads of mini-BAL quasars are much smaller than that of “classical” BAL quasars, it is of interest to make a direct comparison between PC 1415+3408 and BAL quasars in light of a unified model of the BAL phenomenon. In the 72 BAL quasar spectra observed by Korista et al. (1993) at resolution 2.1 \AA , only two objects have zero flux in the C IV absorption profile. Of the 58 Korista et al. spectra that cover N V and Ly α , none have black N V absorption, even when the N V profiles are saturated.

Black absorption troughs imply that the absorbing material is being viewed from a direction where both the broad emission line region and the continuum sources are fully occulted by the BAL material and there is virtually no scattering back into the line of sight. Since black saturation is virtually never seen in BAL quasars, this suggests that we are either seeing PC 1415+3408 at a low probability viewing angle, or that the BAL flow geometry around this quasar is not common to BAL quasars. For BALs originating from an equatorial flow (e.g. Emmering, Blandford, & Shlosman 1992; Murray et al. 1995; de Kool & Begelman 1995), two low-probability viewing angles include one *directly* edge on to the disk or one grazing the BAL flow material right at the opening angle. However, a line of sight grazing the opening angle might be more likely to have residual flux in the absorption trough due to partial coverage of the compact continuum source or due to light scattered back into the line of sight or to a non-unity filling factor of BAL material. It might be that the

spatial extent or cross section of any scattering material is diminutive. On the other hand, an edge-on viewing angle might be difficult to understand in view of the larger overall velocity spread predicted by some models for such an orientation (e.g. see Fig. 5b of Murray et al. 1995). Whatever the viewing angle, the kinematics of the Ly α absorption and the presence of N V and C IV detached troughs suggest that the BAL flow material does not have uniform ionization and/or density structure.

The velocities of the secondary, or detached troughs, are $-3500 \leq v \leq -2200 \text{ km s}^{-1}$ for N V and $-5000 \leq v \leq -3000 \text{ km s}^{-1}$ for C IV (see Fig. 7). Though they are narrower, these troughs are more typical of the non-black, flat-bottomed, saturated profiles seen in higher velocity BALs (e.g. Arav et al. 1998). Since the detached N V trough is at a lower velocity than the detached C IV trough, the ionization condition may decrease with outflow velocity. This is contradictory to models that predict constant ionization [see de Kool (1997) and references therein] or increasing ionization (e.g. Murray et al. 1995) with outflow velocity. For the N V, either the continuum source is not absorbed (occulted) or the trough is significantly filled in by photons. The latter would imply that any material that scatters light back into the line of sight would be at relatively high velocities with respect to the quasar. It should be noted that there is absorption structure along the red wing of the Ly α emission line that may be due to even higher velocity N V gas (see upper panel of Figure 6). In the case of C IV, at least part of the continuum source is absorbed, or the source of photons filling in the

absorption trough is not as strong as for the N V.

Double-trough broad absorption from C IV has been investigated as a possible signature of line-driven radiation pressure. Since all absorbing species experience the same flow, they each have the same optical depth modulation, showing a reduced optical depth due to increased flux from the Ly α emission line. The so-called “ghost of Ly α ” effect (Turnshek et al. 1988; Arav 1997) corresponds to a “hump” in the C IV absorption at $v \sim -5900 \text{ km s}^{-1}$, the velocity of the Ly α emission peak in the rest-frame of N V ions. Given the exceptionally strong N V absorption, PC 1415+3408 is a good candidate for exhibiting this modulation if the material is driven by radiation pressure. The ghost of Ly α effect is not seen in PC 1415+3408; however, we point out that the C IV absorption terminates at $\sim -5000 \text{ km s}^{-1}$ and that this termination could be induced by the effect.

6. THE PROMISE OF MINI-BAL QUASARS

Despite significant efforts, the overall multi-band statistical properties of quasars exhibiting BAL flows are not yet on a solid statistical footing. Overall, BAL quasars are radio-quiet (e.g. Stocke et al. 1992) and quiet, or self-absorbed, in soft X-rays (Kopko, Turnshek, & Espey 1994; Green & Mathur 1996). However, the FIRST Survey has produced examples of radio-selected, radio-loud BAL quasars (Becker et al. 1997), and there are now a few X-ray loud BAL quasars observed in hard X-rays (e.g. Mathur, Elvis, & Singh 1995; Gallagher et al. 1999; and see predictions of Krolik & Voit 1998). For radio-loud BAL quasars, the radio spectra have a range of spectral indices (e.g. Barthel, Tytler, & Vestegaard 1997; Becker et al. 1997), and it is not unexpected that X-ray spectra

would as well.

The X-ray spectra of Mini-BAL quasars may be a key for understanding BAL flows. For example, assuming radiation pressure driven flow dynamics, Murray et al. (1995) predict that quasars with harder (flatter) X-ray spectra, will have wind terminal velocities no greater than $\sim 5000 \text{ km s}^{-1}$. Flatter X-ray spectra might naturally explain the sub-population of Mini-BAL quasars, if the flow dynamics are governed by the energy index, α_E , of the X-ray spectrum. Mini-BALs may provide the first robust measurements of or limits on the X-ray spectral energy indices, especially using more powerful, forthcoming X-ray observatories (AXAF and XMM). Both deeper radio and hard X-ray observations of Mini-BAL quasars at all redshifts could be very telling for constraining unified models of quasars. At the highest redshifts, PC 1415+3408 appears to be a good target for such investigations.

We especially thank Niel Brandt for many fruitful discussions on BAL quasar and X-ray properties and David Turnshek for comments that led to a much improved manuscript. We also thank Roger Blandford, Jane Charlton, George Chartas, Mike Eracleous, and Sarah Gallagher for helpful discussions, and Rajib Ganguly for use of his code to compute partial covering factors. Robert Deverill and David Saxe created much of the software for the data processing and George Weaver provided valuable computing support. This work has been supported in part by National Science Foundation Grants AST96-17185 (CWC), AST95-09919 (DPS), AST94-15574 (MS), AST86-18257A02 (JEG), and by NASA LTSA Grant NAG5-6399 (CWC).

REFERENCES

- Aldcroft, T., Bechtold, J., and Foltz, C. 1997, in Mass Ejection from AGN, ASP Conference Series 28, eds. N. Arav, I. Shlosman, and R. J. Weymann, (PASP : San Francisco), 25
- Anderson, S. F., Weymann, R. J., Foltz, C. B., Chaffee, Jr., F. H. 1987, AJ, 94, 278
- Arav, N. 1996, ApJ, 456, 617
- Arav, N., in Mass Ejection from AGN, ASP Conference Series 28, eds. N. Arav, I. Shlosman, and R. J. Weymann, (PASP : San Francisco), 208
- Arav, N., Korista, K. T., de Kool, M., Junkkarinen, V., and Begelman, M. 1998, ApJ, submitted (astro-ph/9810309)
- Arav, N., Shlosman, I., and Weymann, R. J. 1997, Mass Ejection from AGN, ASP Conference Series 28, (PASP : San Francisco)
- Barlow, T. A., Hamann, F., and Sargent, W. L. W. 1997, in Mass Ejection from AGN, ASP Conference Series 28, eds. N. Arav, I. Shlosman, and R. J. Weymann, (PASP : San Francisco), 13
- Barlow, T. A., and Sargent, W. L. W. 1997, ApJ, 113, 136
- Barthel, P. D., Tytler, D. R., and Vestegaard, M. 1997, in Mass Ejection from AGN, ASP Conference Series 28, eds. N. Arav, I. Shlosman, and R. J. Weymann, (PASP : San Francisco), 48
- Becker, R. H., et al. 1997, in Mass Ejection from AGN, ASP Conference Series 28, eds. N. Arav, I. Shlosman, and R. J. Weymann, (PASP : San Francisco), 31
- Briggs, F. H., Turnshek, D. A., and Wolfe, A. M. 1984, ApJ, 287, 549
- Cohen, M. H., Ogle, P. M., Tran, H. D., Vermeulen, R. C., Miller, J. S., Goodrich, R. W., and Martel, A. 1995, ApJ, 448, L77
- Churchill, C. W. 1997, Ph.D. Thesis, University of California, Santa Cruz
- de Kool, M. 1997, in Mass Ejection from AGN, ASP Conference Series 28, eds. N. Arav, I. Shlosman, and R. J. Weymann, (PASP : San Francisco), 233
- de Kool M., and Begelman, M. C. 1995, ApJ, 455, 448
- Emmering, R. T., Blandford, R. D., and Shlosman, I. 1992, ApJ, 385, 460
- Gallagher, S. C., Brandt, W. N., Sambruna, R. M., Mathur, S., and Yamasaki, N. 1999, ApJ, in press (astro-ph/9902045)
- Ganguly, R., Eracleous, M. C., Charlton, J. C., and Churchill, C. W. 1999, AJ, submitted
- Goodrich, R. W. 1997, in Mass Ejection from AGN, ASP Conference Series 28, eds. N. Arav, I. Shlosman, and R. J. Weymann, (PASP : San Francisco), 94
- Green, P. J., and Mathur, S. 1996, ApJ, 462, 637
- Green, P. J., et al. 1995, ApJ, 450, 51
- Gunn, J. E., and Peterson, B. A. 1965, ApJ, 142, 1633
- Giallongo, E., and Cristiani, S. 1990, MNRAS, 247, 696
- Hamann, F. 1997, ApJS, 109, 279
- Hamann, F., Barlow, T. A., Beaver, E. A., Burbidge, E. M., Cohen, R. D., Junkkarinen, V., and Lyons, R. 1995, ApJ, 443, 606
- Hamann, F., Barlow, T. A., and Junkkarinen, V. 1997a, ApJ, 478, 87
- Hamann, F., Barlow, T. A., Junkkarinen, V., and Burbidge, E. M. 1997b, ApJ, 478, 80
- Hamann, F., Beaver, E. A., Cohen, R. D., Junkkarinen, V., Lyons, R., and Burbidge, E. M. 1997c, ApJ, 488, 155

- Horne, K. 1986, *PASP*, 98, 609
- Jenkins, E. B., and Ostriker, J. P. 1991, *ApJ*, 376, 33
- Kellerman, K. I., Sramek, R., Schmidt, M., Green, R., and Shaffer, D. B. 1984, *AJ*, 108, 1163
- Kellerman, K. I., Sramek, R., Schmidt, M., Shaffer, D. B., and Green, R. 1989, *AJ*, 98, 1195
- Kopko, M., Turnshek, D. A., and Espey, B. 1994, in *IAU Symp.* 159, *Quasars Across the Electromagnetic Spectrum*, eds. T. J.-L. Courvoisier & A. Blencha (Dordrecht: Kluwer), 450
- Korista, K. T., Voit, G. M., Morris, S. L., and Weymann, R. J. 1993, *ApJS*, 88, 357
- Krolik, J. H., and Voit, G. M. 1998, *ApJ*, 497, L5
- Mukai K. 1997, *PIMMS Users' Guide*. NASA/GSFC, Greenbelt
- Mathur, S., Elvis, M., and Singh, K. P. 1995, *ApJ*, 455, L9
- More, J. J. 1978, in *Numerical Analysis Proceedings*, ed. G. A. Watson, (Springer-Verlag), 630
- Morris, S. L., Weymann, R. J., Foltz, C. B., Turnshek, D. A., Shethman, S., Proce, C., and Boroson, T. A. 1986, *ApJ*, 310, 40
- Murray, N., Chiang, J., Grossman, S. A., and Voit, G. M. 1995, *ApJ*, 451, 498
- Oke, J. B., et al. 1995, *PASP*, 107, 375
- Oke, J. B., and Gunn, J. E. 1983, *ApJ*, 266, 713
- Oke, J. B., and Korycanski, D. G. 1982, *ApJ*, 255, 11
- Sargent, W. L. W., Boksenberg, A., and Steidel, C. C., 1988, *ApJS*, 68, 539
- Savage, B. D., and Sembach, K. R. 1991, *ApJ*, 379, 245
- Schneider, D. P., Schmidt, M., and Gunn, J. E. 1991, *AJ*, 101, 2004
- Schneider, D. P., Schmidt, M., and Gunn, J. E. 1989, *AJ*, 98, 1507
- Schneider, D. P., Schmidt, M., and Gunn, J. E. 1997, *AJ*, 114, 36 (SSG97)
- Schmidt, M., Schneider, D. P., and Gunn, J. E. 1995, *AJ*, 110, 68
- Schmidt, M., van Gorkom, J. H., Schneider, D. P., and Gunn, J. E. 1995, *AJ*, 109, 473
- Stark A. A., Gammie C. F., Wilson R. W., Bally J., Linke R., Heiles C., Hurwitz M. 1992, *ApJS*, 79, 77
- Stoeckle, J. T., Morris, S. L., Weymann, R. J., and Foltz, C. B. 1992, *ApJ*, 396, 487
- Storrie-Lombardi, L. J., MacMahon, R. G., Irwin, M. J., and Hazard, C. 1996, *ApJ*, 468, 121
- Turnshek, D. A., 1984, *ApJ*, 280, 51
- Turnshek, D. A., 1988, in *QSO Absorption Lines: Probing the Universe*, ed. J. C. Blades, D. A. Turnshek, & C. A. Norman, (Cambridge : Cambridge University Press), 17
- Turnshek, D. A., 1988, Foltz, C. B., Grillmair, C. J., Weymann, R. J. 1988, *ApJ*, 325, 651
- Turnshek, D. A., 1995, in *QSO Absorption Lines*, ed. G. Meylan, (Springer-Verlag : Garching), p 223
- Turnshek, D. A., Koptko, Jr., M., Monier, E., Noll, D., Espey, B. R., and Weymann, R. J. 1996, *ApJ*, 463, 110
- Turnshek, D. A., 1997a, in *Mass Ejection from AGN*, ASP Conference Series 28, eds. N. Arav, I. Shlosman, and R. J. Weymann, (*PASP* : San Francisco), 52
- Turnshek, D. A., 1997b, in *Mass Ejection from AGN*, ASP Conference Series 28, eds. N. Arav, I. Shlosman, and R. J. Weymann, (*PASP* : San Francisco), 193
- Weymann, R. J. 1995, in *QSO Absorption Lines*, ed. G. Meylan, (Springer-Verlag: Garching), 213
- Weymann, R. J., Carswell, R. F., and Smith, M. G. 1981, *ARA&A*, 19, 41
- Weymann, R. J., Morris, S. L., Foltz, C. B., and Hewitt, P. C. 1991, *ApJ*, 373, 23
- Weymann, R. J., and Williams, R. E., *Phys. Scripta*, 17, 217
- Wilkes, B. J., and Elvis, M. 1987, *ApJ*, 323, 243
- Williams, R.E., et al. 1992, *ApJ*, 389, 157